Many-body potentials and atomic-scale relaxations in noble-metal alloys

G. J. Ackland* and V. Vitek
Department of Materials Science and Engineering, University of Pennsylvania, Philadelphia, Pennsylvania 19104-6272
(Received 10 March 1989; revised manuscript received 30 October 1989)

We derive empirical many-body potentials for noble-metal alloy systems in the framework of the Finnis-Sinclair model [Philos. Mag. A **50**, 45 (1984)] which is based on a second-moment approximation to the tight-binding density of states for transition metals [F. Cyrot, J. Phys. Chem. Solids **29**, 1235 (1968)]. The most important extension of the model is a simple incorporation of interspecies interactions which involves fitting the alloying energies. The importance of properly accounting for the local atomic relaxations when constructing the potentials is emphasized. The observed principal features of the phase diagrams of the alloys are all well reproduced by this scheme. Furthermore, reasonable concentration dependences of the alloy lattice parameter and elastic constants are obtained. This leads us to suggest that fine details of the electronic structure may be less important in determining atomic structures than are more global parameters such as atomic sizes and binding energies.

I. INTRODUCTION

Empirical descriptions of interatomic forces have been widely used in simulations of extended lattice defects such as grain boundaries, dislocations, clusters of point defects, etc.[1] A significant recent advancement in the empirical descriptions of interatomic forces has been the introduction of many-body terms in addition to pairwise potentials. These terms model the effect of the local electronic density. Two schemes of this type, the "embedded-atom method" (EAM) of Daw and Baskes[2,3] and Finnis and Sinclair potentials[4] (referred to as FS), although based on rather different approaches, yield strikingly similar models in the case of pure metals. Both of these models are fitted so as to reproduce the lattice parameter, cohesive and vacancy-formation energies, and elastic constants. They have been shown to give very good results in simulations of point defects, cracks, and surfaces,[2-19] three applications for which traditional pair potentials are known to be inadequate. In numerous other applications, these and other many-body potentials have yielded reasonable results, generally similar to those obtained earlier using pair potentials.

Given the success of these new potentials in the case of pure metals, a natural development is to extend these schemes to alloys and several attempts have already been made in the framework of the EAM. The formalism of the EAM, indeed, appears to be most directly applicable. In this model the total energy of a system is written as a sum of two terms,

$$E=\sum_i F_i(\rho_i)+\tfrac{1}{2}\sum_{i,j} V_{ij}(R_{ij}) , \tag{1}$$

where

$$\rho_i=\sum_j \Phi_j(R_{ij}), \quad V_{ij}=\frac{Z_i Z_j}{R_{ij}} .$$

The many-body term here is given by a function, F_i, of a local electron density ρ_i. The functional form of F_i is dependent only upon the species of the embedded atom (atom i) and not on the species of its neighbors. ρ_i, on the other hand, is the electron density due to the surrounding atoms, and is a sum of one-atom contributions, Φ_j, independent of the species of the embedded atom. Likewise, the EAM pairwise potential V_{ij} can be separated into a product of two one-atom functionals Z_i and Z_j, although some more recent EAM-type models[20,21] have used nonseparable forms for the pair potential. Thus the total energy can be written in terms of functional forms, each of which is dependent on one atom only, and thus independent of the alloy in which the atom is present. Consequently, in principle, using the EAM, alloy properties could be derived directly from parameters for pure metals. Although this is a lot to hope for, it is not entirely unreasonable to aim for, since good predictions of alloy structures have been obtained from pure-metal parameters using empirical schemes.[22-24] Unfortunately, it was found that direct application of EAM parameters derived for pure materials leads to poor results for the formation enthalpies and volumes of the corresponding alloys.[25] A set of EAM functions for a variety of different fcc metals and alloys have been derived, but only by refitting to properties of the alloys.[26,27]

The FS model[3] appears to be less convenient for direct conversion from pure metals to alloys. In this model the expression for the total energy of the system is similar to the EAM, but the many-body term is given by a square root of a sum of two-body potentials, i.e., $F_i=-\sqrt{\cdots}$, and both V and Φ are dependent on the species of both atoms i and j, and thus they are not directly transferable from a pure metal to an alloy. Other many-body potential schemes[19] also contain similar two-center terms. Thus it appears that none of the many-body potential schemes can provide potentials for alloys without further empirical fitting to properties of those alloys. We acknowledge this, and while starting with the potentials for

pure metals developed within the FS scheme[17] (see Appendix A), we proceed to derive many-body potentials for alloys by carrying out an additional fitting to alloying energies of random alloys.

The many-body potentials are constructed in this paper for alloys of the noble metals Au, Ag, and Cu. These alloys provide an interesting variety of systems: silver-gold forms a disordered fcc-based alloy throughout its concentration range, copper-silver shows only a limited solid solubility governed by the entropy effect, while copper-gold forms a variety of ordered alloys. When constructing the potentials, we address the question of local relaxation of atoms in disordered substitutional alloys. This is shown to be a significant effect, which has to be properly accounted for in the fitting procedure. However, it can only be fully incorporated by carrying out extensive combined molecular-dynamics and Monte Carlo calculations. We examine, therefore, several different approximations and show that there may be significant differences between them. Hence, for different alloy systems different approximations need to be chosen, using the alloying behavior known from the corresponding phase diagram as a guideline.

We demonstrate that constructed potentials reproduce the basic features of the phase diagrams which are in agreement with experiments and first-principles calculations.[28,29] They also lead to reasonable concentration dependences of the lattice parameters and elastic constants which agree with experimental data where available.

II. FORM OF THE POTENTIALS

The FS potential formalism is based on a second-moment approximation to the tight-binding theory[30] incorporating charge conservation.[31,32] This gives rise to a many-body cohesive term in the form of a square root of a sum of pairwise terms. For a pure metal the energy of an atom i can thus be written

$$E_i=\frac{1}{2}\sum_j V(R_{ij})-\left[\sum_j \Phi(R_{ij})\right]^{1/2}, \tag{2}$$

where the summation extends over all the atoms. V is a pair potential which is strongly repulsive for small separations of atoms. Φ can be interpreted as a sum of squares of hopping integrals within the tight-binding approach.

In an extension of the model to alloys, both V and Φ are dependent on the species of the atoms at i and j. The species dependence is thus inseparable. A consequence of this inseparability is that for an N-component system we need $\sum_{i=1}^{N} i$ different two-center functions V and Φ. For a similar system the EAM requires only N different functions for F, ρ, Φ, and Z, one for each species. In the present work we study binary systems, so we need three different functions for both V and Φ. We will denote these functions V_{AA}, V_{AB}, V_{BB}, Φ_{AA}, Φ_{AB}, and Φ_{BB}, where the suffices refer to the species of the atoms involved.

In keeping with the original FS model and its subsequent extension to noble metals,[17] it was desired that the empirical functions should take a simple analytic form. We assumed that each of these functions is independent of the concentration of the alloys. Hence functions V_{AA}, V_{BB}, Φ_{AA}, and Φ_{BB} were identified with those for pure metals and taken from previous work,[17] with the exception of copper,[33] as explained in Appendix A. The function Φ_{AB} was chosen as a geometrical mean of Φ_{AA} and Φ_{BB}. This is consistent with its interpretation in terms of hopping integrals, and minimizes the empirical fitting. Hence, five of the six empirically fitted functions are determined from the pure-metal properties and only the pair potential V_{AB} has been fitted to alloy properties.

Previous works[26,34] have usually used the energy of a single substitutional atom for empirical fitting of alloying energies. This gives two experimental data to which to fit for each binary system. The advantage of this property is that it is easy to calculate theoretically but there are a number of drawbacks which are seldom discussed. First, experimental data for single substitutional atoms do not exist as such. The data usually used are extrapolated from a region of about 10% concentration. At this concentration 72% of impurity atoms have at least one impurity as a nearest neighbor (based on a random distribution of species in a fcc lattice), and less than one impurity in 10^{11} can be regarded as isolated, assuming the interaction of atoms extends up to the third neighbors. Second, the effects of relaxation of the lattice around the impurity are known to be significant. The nature of this relaxation will be different for an atom in a 10% alloy than for an isolated impurity. Therefore, in this work we fit V_{AB} to observed random-alloy formation enthalpies at finite concentrations.[35] Since the calculation of properties of random alloys is not straightforward when taking into account the local relaxation, we shall discuss this in detail in the following section. The fitting is then described separately for each system studied because the nature of the fitted data varies between the three alloy systems.

For consistency with the functional forms used for the pure materials, we employed cubic splines for V_{AB}. This is, of course, an arbitrary choice based on computational convenience. This ensures smooth derivatives up to the second order and can, therefore, be expected to be good when considering first-order (energies) and second-order effects (relaxations and elastic constants). However, to examine third-order effects, such as thermal expansion or Grüneisen constants, functions with smooth third derivatives are needed, and the present potentials are thus not suitable for such studies.

The functions which make up the present model are

$$\begin{aligned}
V_{AA}(R_{ij})&=\sum_{k=1}^{6} a_k^{AA}H(r_k^{AA}-R_{ij})(r_k^{AA}-R_{ij})^3 ,\\
\Phi_{AA}(R_{ij})&=\sum_{k=1}^{6} A_k^{AA}H(R_k^{AA}-R_{ij})(R_k^{AA}-R_{ij})^3 ,\\
V_{AB}(R_{ij})&=\sum_{k=1}^{3} a_k^{AB}H(r_k^{AB}-R_{ij})(r_k^{AB}-R_{ij})^3 ,\\
\Phi_{AB}(R_{ij})&=\sqrt{\Phi_{AA}(R_{ij})\Phi_{BB}(R_{ij})} ,
\end{aligned} \tag{3}$$

TABLE I. Parameters for potentials V_{AB}.

A	B	r_1 (Å)	r_2 (Å)	r_3 (Å)	a_1 (eV/Å^3)	a_2 (eV/Å^3)	a_3 (eV/Å^3)
Ag	Au	4.408 56	3.469 70	3.000 00	0.003 566 503 525	1.015 075 326	0.000 000 00
Au	Cu	4.309 816	4.047 479	3.297 946	−0.085 545 516 60	0.192 835 880	0.759 322 86
Ag	Cu	4.158 00	3.157 00	3.000 00	0.035 330 377 52	0.851 846 635 3	0.000 000 00

where $H(x)$ is the Heaviside unit-step function which gives the cutoff distance of each spline segment. V_{BB} and Φ_{BB} have the same form as the functions V_{AA} and Φ_{AA}. While V_{AA} is a six-point cubic spline, a three-point spline for V_{AB} was found to be sufficient to reproduce the experimental data fitted (alloying energies). The parameters A_k^{AA}, a_k^{AA}, R_k^{AA}, and r_k^{AA} are identical to those determined for pure materials (see Appendix A). The parameters a_k^{AB} and r_k^{AB} for the function V_{AB}, determined for the three alloy systems as described below, are summarized in Table I. For pure metals these coefficients are given in a normalized form, but for alloys there is no unique lattice parameter for all concentrations with respect to which one can define the coefficients, so in Table I we use absolute units of angstroms and eV/Å^3 for r_k^{AB} and a_k^{AB}, respectively.

III. APPROXIMATE MODELS OF RANDOM ALLOYS

Since we wish to fit our potentials to alloying energies of random alloys, it is necessary to have a simple method for calculating these energies. There have been numerous models to describe a random alloy based on a fcc lattice, but none of them treats accurately the local relaxation. This can, of course, be fully accounted for by carrying out combined molecular-statics (or -dynamics) and Monte Carlo calculations, but such an approach is too computationally expensive to be used iteratively in the fitting process at various alloy concentrations. Hence, we employ approximations, and three different possibilities are discussed below. The molecular statics has been used only as a check on the already derived potentials. For this purpose we employed the molecular-dynamics (MD) program MOLDY (Ref. 10) adapted for use in quenched MD and, therefore, suitable as a molecular-statics program. We examined sample blocks containing 256 atoms and 500 atoms with periodic boundary conditions.

In all cases we consider a fcc lattice with two types of atoms, A and B, present with atomic fractions c_A and c_B. For each approximation we determine the energy per atom in the random alloy, E^{rand}, and the alloying energy is then

$$E^{\text{alloy}}=E^{\text{rand}}-c_A E^A-c_B E^B , \tag{4}$$

where E^A and E^B are energies per atom in the pure metals A and B, respectively. The available experimental data on alloying energies frequently correspond to high temperatures, while no temperature effects are taken into account in fitting procedures. Hence, we are here adopting an approximation that the alloying energy is independent of temperature below the melting point.

A. Total smearing model

The total smearing model (TSM) is the simplest analytic model for a random alloy, and that which makes the most severe approximations. Each site is regarded as occupied by a particle consisting of a fraction c_A of an A atom and a fraction c_B of a B atom. This can be regarded as a smearing out of both atomic types at each site. This description has been used frequently, for example, in a previously developed pair-potential model for alloys of noble metals[34] and it is equivalent to the regular-solution model. The lattice has perfect cubic symmetry, with all sites identical, and so it will not relax locally. The lack of local relaxation makes the predicted energy of the TSM too high. However, since all atoms are regarded as being in regions of perfect stoichiometry, the mixing of the species is overcomplete (i.e., regions rich in one species or the other are not considered). The energy per atom in this approximation is

$$\begin{aligned} E^{\text{rand}}= & c_A^2\sum_j V_{AA}(R_{ij})+c_B^2\sum_j V_{BB}(R_{ij}) \\ & +2c_Ac_B\sum_j V_{AB}(R_{ij}) \\ & -\left[c_A^2\sum_j \phi_{AA}(R_{ij})+c_B^2\sum_j \Phi_{BB}(R_{ij})\right. \\ & \left.+2c_Ac_B\sum_j \Phi_{AB}(R_{ij})\right]^{1/2} , \end{aligned} \tag{5}$$

and the lattice parameter is determined by minimizing this energy for a given alloy concentration.

This model can be improved by regarding the species of an atom i as fixed and taking only its neighbors as smeared. In this way the central atom has a distinct species, but its surroundings consist of smeared atoms as in the TSM. There are thus two distinct types of site, A and B, but they are both embedded in the same environment. This again means that no local relaxation is permitted and the mixing is overcomplete. The average lattice parameter is determined by minimizing the energy per atom which is, in this case,

$$\begin{aligned} E^{\text{rand}}= & c_A^2\sum_j V_{AA}(R_{ij})+c_B^2\sum_j V_{BB}(R_{ij}) \\ & +2c_Ac_B\sum_j V_{AB}(R_{ij}) \\ & -c_A\left[c_A\sum_j \Phi_{AA}(R_{ij})+c_B\sum_j \Phi_{AB}(R_{ij})\right]^{1/2} \\ & -c_B\left[c_B\sum_j \Phi_{BB}(R_{ij})+c_A\sum_j \Phi_{AB}(R_{ij})\right]^{1/2} . \end{aligned} \tag{6}$$

B. Hydrostatic configurational sampling model

In the hydrostatic configurational sampling model (HCSM) there is no smearing and every atom is regarded as being either species A or B with probabilities c_A and c_B, respectively. All possible configurations of atoms around a central atom i are considered. However, no local relaxation is taken into account. Instead, for any given configuration atoms are placed on sites of a perfect lattice with a lattice parameter determined by minimizing the average energy per atom with respect to this lattice parameter. The number of configurations which needs to be sampled depends on the range of interactions. For short-range interactions this number is greatly reduced. Moreover, in the HCSM all atoms in a given shell are regarded as being indistinguishable, so each shell has cubic symmetry. This leads to a considerable amount of degeneracy. For the present third-neighbor model, 4550 possible configurations need to be taken into account.

The total number of degenerate configurations can be written in terms of binomial coefficients. Defining N_n^A as the number of type-A atoms which are nth neighbors of i and Z_n as the total number of neighbors in the nth shell, the probability P_α for any one of the above configurations α is

$$P_\alpha = P(N_1^A, N_2^A, N_3^A, \ldots) = \prod_n \begin{bmatrix} Z_n \\ N_n^A \end{bmatrix} c_A^{N_n^A} c_B^{N_n^B} , \quad (7)$$

where $Z_n = N_n^A + N_n^B$. The energy per atom can then be written in this approximation as

$$E^{\text{rand}} = c_A \sum_\alpha P_\alpha \left[\sum_n [N_n^A V_{AA}(R_n) + N_n^B V_{AB}(R_n)] - \left[\sum_n [N_n^A \Phi_{AA}(R_n) + N_n^B \Phi_{AB}(R_n)] \right]^{1/2} \right]$$
$$+ c_B \sum_\alpha P_\alpha \left[\sum_n [N_n^A V_{AB}(R_n) + N_n^B V_{BB}(R_n)] - \left[\sum_n [N_n^A \Phi_{AB}(R_n) + N_n^B \Phi_{BB}(R_n)] \right]^{1/2} \right] , \quad (8)$$

where the first summation (α) extends over all the possible configurations and the second summation (n) over all the neighboring shells; R_n is the separation of nth neighbors, which, in this case, is the same for all the configurations considered.

C. Local configurational sampling model

The local configurational sampling model (LCSM) is similar to the HCSM, but each of the 4550 configurations in which an atom can be situated is regarded as possessing a local lattice parameter R^α, where α denotes the local atomic configuration. for each of these configurations the energy of the central atom is found by minimization with respect to R^α. Since we do not take into account any local shearing which may arise due to the distribution of different species within a given shell of neighbors, we maintain the same degree of degeneracy as in the HCSM, and keep the cubic symmetry of that model. The energy per atom in this model is

$$E^{\text{rand}} = c_A \sum_\alpha P_\alpha \left[\sum_n [N_n^A V_{AA}(R_n^{A,\alpha}) + N_n^B V_{AB}(R_n^{A,\alpha})] - \left[\sum_n [N_n^A \Phi_{AA}(R_n^{A,\alpha}) + N_n^B \Phi_{AB}(R_n^{A,\alpha})] \right]^{1/2} \right]$$
$$+ c_B \sum_\alpha P_\alpha \left[\sum_n [N_n^A V_{AA}(R_n^{B,\alpha}) + N_n^B V_{AB}(R_n^{B,\alpha})] - \left[\sum_n [N_n^A \Phi_{AB}(R_n^{B,\alpha}) + N_n^B \Phi_{BB}(R_n^{B,\alpha})] \right]^{1/2} \right] . \quad (9)$$

This is similar, as in the previous case [Eq. (8)], but the separations of the nth neighbors, $R_n^{A,\alpha}$ and $R_n^{B,\alpha}$, are now different for different configurations.

Although each atom is locally relaxed within all available local configurations, it is not possible to build a crystal out of them without imposing some strains and thereby increasing the energy. Hence, the LCSM overcompensates for the lack of relaxation in the HCSM. Therefore, this model will provide a lower bound to the energy of a random alloy whenever the dominant effect of the relaxation is the radial strain (sometimes called the size effect), while the HCSM will provide an upper bound. In the solid the total local relaxation is impaired by confinement of the local configuration within the surrounding crystal structure. Hence, in this case it is likely that alloying will be better described by the HCSM, although we expect the theoretical values of the alloying energy obtained from the HCSM to be too large, and those from the LCSM to be too small. On the other hand, in the liquid there is no long-range order and thus the confinement of the local configurations is less pronounced. We believe, therefore, that the fully relaxed local configurations of the LCSM will be a better approximation. However, even in the liquid environment, we still expect the LCSM to give too low an alloying energy. In fitting the potentials to alloying energies, we require, therefore, that the experimental values always lie in between those calculated using the HCSM and LCSM ap-

proximations. Which of these approximations is closer depends then on the nature of experimental data, in particular whether they correspond to solids or liquids.

IV. FITTING OF POTENTIALS

A. Silver-gold

The silver-gold phase diagram shows a complete mutual solubility in the solid alloys; no ordered alloys are known to be stable. The alloying energies, corresponding to the solid phase, are available for the whole range of concentrations.[35] Since silver and gold have very similar lattice parameters, it can be expected that the relaxation will be of little importance in this system. Hence, when fitting the alloying energy we described the random alloy using the HCSM, which is a simpler approximation. The experimental data and the fitted dependence of the alloying energy are shown in Fig. 1(a). In the same figure we also show the alloying energy calculated within LCSM using the same potential parameters. It is seen that the results are, indeed, nearly identical and the curves are indistinguishable on the scale of Fig. 1(a). Molecular-statics calculations were carried out for several concentrations and the calculated alloying energies are again practically the same as when using the HCSM or LCSM. Calculations using the TSM gave significantly lower energies (about 40% lower). This gives some measure of the error involved in not sampling the (higher-energy) off-stoichiometric configurations, but it should be noted that fitting was carried out so that the experimental data are always in between the HCSM and LCSM approximations.

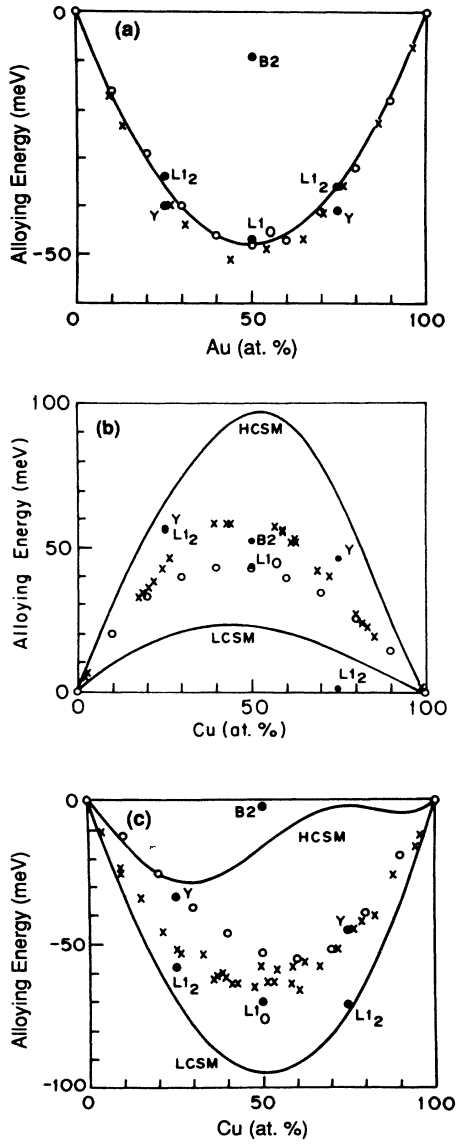

FIG. 1. Concentration dependence of the alloying energy in (a) silver-gold, (b) copper-silver, and (c) copper-gold systems. Calculations using LCSM and HCSM, respectively: solid curves. Experiment: open circles. Molecular-statics calculations: crosses. Ordered alloys: solid circles.

It is interesting to note that some of the molecular statics points lie below the LCSM "lower bound." This is because the radial strains in silver-gold are very small (the atoms have only a 0.2% lattice-parameter mismatch), so the overrelaxation does not affect the alloying energy much; meanwhile, the random distribution in the finite molecular-statics calculation tends to favor near-stoichiometric local configurations (though not as much as the TSM does) and thus the species are overly well mixed, leading to slightly lower energies. This subtle effect is certainly smaller than other approximations which are made (such as the complete lack of local ordering).

B. Copper-silver

Copper-silver alloys have a simple eutectic phase diagram.[35] They exhibit phase separation at 0 K and very limited solid solubility, presumably entropy driven, at higher temperatures. The alloying energies are available across the whole range of concentrations, but only for the liquid phase.[35] For this reason we carried out the fitting such that the experimental data lie between the upper and lower bounds defined by the LCSM and HCSM, but closer to the LCSM curve, as shown in Fig. 1(b). Molecular-statics (MS) calculations based on a fcc lattice lie between the LCSM and HCSM, slightly above the (liquid) experimental data because of the constraints imposed by the lattice. All MS and ordered-alloy calculations on this system suggest that phase separation with entropy-driven solid solubility will be the lowest-energy state.

The TSM gives a still higher energy than the HCSM, because is puts too much weight on the unfavored stoichiometric configuration and does not account for the relaxation.

C. Copper-gold

The copper-gold system has a phase diagram corresponding to various ordered alloys, which undergo an order-disorder transition at high temperatures.[35] For this reason the alloying energies for random alloys, to which we fit V_{AB}, are only available for high temperatures, and thus we again use the approximation of temperature in-

dependence of the alloying energy. These data correspond to the solid phase and, therefore, we carried out the fitting such that the experimental data lies in between the upper and lower bounds defined by the LCSM and the HCSM, as shown in Fig. 1(c). Furthermore, the lattice parameter for the ordered Cu_3Au alloy was fitted since the potentials are intended for studies of lattice defects in this alloy.

Molecular-statics calculations were carried out for wide range of concentrations and their results are also shown in Fig. 1(c). They follow the experimental values very closely for copper concentrations larger than 50%, but for gold-rich alloys the calculated values are lower than the experimental ones, closer to values calculated using LCSM. This means that in the latter case the local relaxations obtained using the potentials are more extensive than in the real alloy. However, a short-range order is likely to exist in reality, even at high temperatures, which suppresses the relaxation, while the fitting was carried out assuming an ideally disordered alloy.

The TSM gives results between the LCSM and HCSM curves. The lack of relaxation make the TSM value too low, but the excess weight on favored perfect stoichiometry makes it too high. In this system these errors roughly cancel.

V. CALCULATED PROPERTIES OF ALLOYS: TEST OF POTENTIALS

A. Alloy structures

The first test of the validity of the constructed potentials is how well they reproduce the main features of the phase diagrams of the alloy systems studied. For this purpose we evaluated for each system alloying energies of ordered alloys corresponding to concentrations 50%-50% and 25%-75%. These are the bcc-based $B2$ structure, the fcc-based $L1_2$ and $L1_0$ structures, and a structure we mark "Y". The Y structure is a theoretically constructed crystal structure which can be regarded as a faulted $L1_2$ structure with repeated $\frac{1}{2}[011](111)$ stacking faults. The mathematical significance of this crystal structure is that it maximizes the number of unlike second neighbors. Corresponding calculated alloying energies are shown in Figs. 1(a)–1(c).

In the Au-Ag system the alloying energies of $L1_2$, $L1_0$, and Y structures are very close to those of the corresponding disordered alloys while the $B2$ structure has an appreciably higher energy. The lowest-energy structure appears to be the Y structure, but even in this case the difference in the energy between the ordered and disordered state is only about 4.5 meV, corresponding to the thermal energy of about 20 K. Hence, the ordering energies are very small, and in view of the approximations made in the model we consider them to be negligible. Thus the random alloy will be stabilized by the entropy contribution to the free energy at practical temperatures. Furthermore, even if the ground state is an ordered structure at low temperature, this structure may never be attained because the kinetic barriers involved in the transformation are too great to be overcome at low temperature. This is in agreement with the observation that Au-Ag alloys are always disordered.

The alloying energies of the ordered alloys evaluated for the Cu-Ag system are all positive, although the energy of the Cu_3Ag $L1_2$ alloy is, within the limits of the present model, zero. Similarly, the alloying energies of disordered alloys are all positive. This implies that both ordered and disordered alloys of copper and silver are for all concentrations unstable with respect to the separation. This is indeed observed for the solid state.

The situation is different in the Cu-Au system. The alloying energies of $L1_2$ Cu_3Au and Au_3Cu alloys, as well as of the $L1_0$ CuAu alloy are lower than those of the corresponding disordered alloys and/or $B2$- and Y-ordered alloys. Hence, these ordered structures are favored at low temperatures over both the disordered phase and $B2$- or Y-ordered structures, as observed.[35] We have not attempted to calculate the order-disorder transition temperatures. These depend very sensitively on both the ordering energies and the treatment of the entropy, which must incorporate possible short-range order in the disordered state. However, we have evaluated the energy of the $\frac{1}{2}\langle 110\rangle$ antiphase boundary on the $\{111\}$ planes in Cu_3Au, which is a more global quantity principally controlled by the ordering energy. It was found to be 53 mJ m^{-2}, which compares well with the experimental estimates[36,37] of 40–60 mJ m^{-2}.

An interesting feature of the dependence of the alloying energy of disordered alloys on concentration is that the minimum or maximum is displaced away from the 50%-50% mixture in the case of Cu-Ag and Cu-Au alloys. In calculations this is replicated for the Cu-Ag alloys when using the LCSM but not the HCSM approximation, which suggests that this phenomenon is related to the relaxation. In this case the peak is displaced toward Ag-rich alloys and this can be understood in terms of the size difference between the atoms. The effect of large Ag atoms being forced into small spaces between Cu atoms is reduced by the relaxation more than when small Cu atoms are placed in between larger Ag atoms. The displacement of the minimum towards Au-rich Cu-Au alloys can be understood in the same terms, but it is a weaker effect and the LCSM approximation reproduces it only marginally. No such effect occurs in Au-Ag alloys, where there is a negligible size difference between the two elements.

Alloying behavior in noble-metal alloys has recently been investigated using an augmented-spherical-wave–(ASW-) based density-functional-theory model[28] to calculate ground-state energies and a cluster-variation method to investigate the entropy effect on the order-disorder phase transition.[29] While our model cannot be expected to reproduce these results quantitatively, qualitatively it gives very similar results to these more fundamental calculations. This encourages us to believe that it will be sufficiently accurate in calculations which are beyond the scope of *ab initio* methods, such as studies of extended defects in which atomic relaxations need to be fully accounted for.

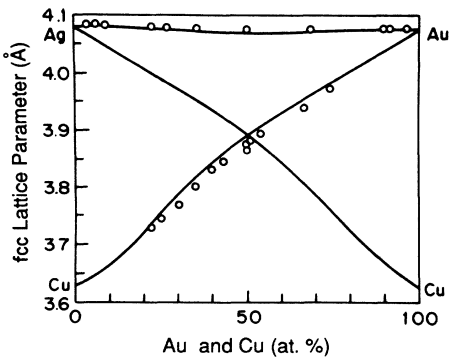

FIG. 2. Concentration dependence of the lattice parameter in random alloys. Calculations: solid curves. Experiment: open circles.

B. Lattice parameters and elastic constants

The calculated dependences of the lattice parameters of the disordered alloys studied are shown in Fig. 2 as solid curves. These dependences exhibit only small deviations from Vegard's law, and comparison with available experimental data,[38] which are also shown in this figure, reveals that the sense of these deviations agrees with these data. These curves are derived from a quintic polynomial fitted to the results of the molecular-statics calculation. The lattice parameter is insensitive to the method used to describe the alloy—TSM, LCSM, and HCSM approximations lead to very similar curves.

The concentration dependences of the elastic constants of the disordered alloys were calculated for Au-Ag and Cu-Au systems using the LCSM approximation, and these are shown in Figs. 3(a) and 3(b). Since no solid disordered Cu-Ag alloy exists, calculations were not made for this system. It is shown in Appendix B that in the framework of the many-body potentials employed here a relationship exists between the pair-potential contributions to the elastic constants of alloys, so that the alloy elastic constants could not be fitted independently. No such fit was, of course, attempted here. However, since no fitting is achievable in principle, a correct prediction of the concentration dependence of the elastic constants would represent a good confirmation of the validity of the potentials. Unfortunately, measurements of elastic constants in alloys are very rare. From the alloys studied here more extensive experimental data are available only for the Au-Ag system;[39] they are shown in Fig. 3(a). However, these measurements have been made at high temperatures, while the fitting of potentials for both pure metals and alloys was carried out for the case of 0 K. For this reason the experimental data shown in Fig. 3(a) are somewhat lower than the calculated values even for pure Au and Ag. Nevertheless, this comparison demonstrates that both the values of the elastic constants and their concentration dependence are well reproduced by the constructed potentials. For Cu-Au the only available data are for the 3:1 disordered alloy[39] and these are in agreement with calculations, even though the measurements were again carried out at high temperatures.

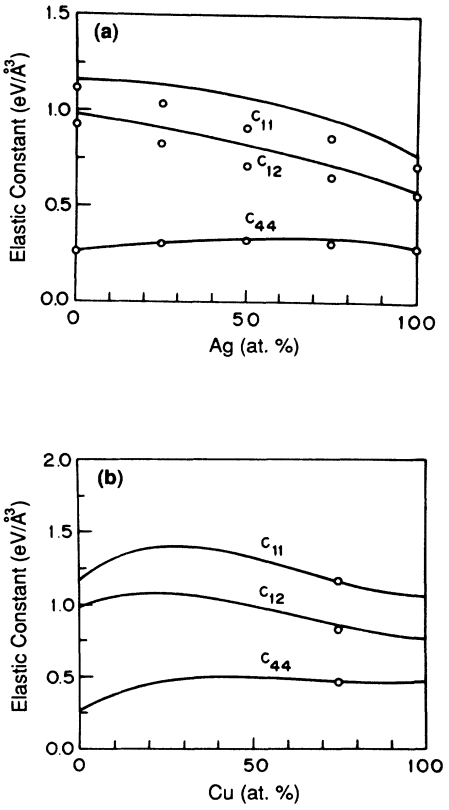

FIG. 3. Concentration dependence of elastic constants in random alloys: (a) gold-silver and (b) gold-copper. Calculated values: solid curves. Experiment: open circles.

C. Isolated substitutional impurities

Using constant-pressure molecular-statics calculations we evaluated the energy associated with a single substitutional impurity atom in a host of another element. This quantity is useful when examining various segregation properties. It has also been commonly used in fitting of empirical potentials. By comparison, with extrapolated data from molecular-statics calculations we show that the error introduced by assuming that data from a 10% concentration can be applied to calculations of truly isolated impurities is quite significant. The calculated energies of isolated substitutional atoms, both before and after relaxation of the host lattice, and data extrapolated from the molecular-statics curves at 10% concentration (the lowest experimentally published data) are presented in Table II. The extrapolation was taken from a quintic polynomial fit to the molecular-statics data which were constrained to pass through a mixing enthalpy of zero at 0% and 100% concentrations (cf. Fig. 1). A discrepancy of up to 15% arises between the extrapolation of the molecular-dynamics data and the calculation carried out for a completely isolated impurity. This shows that even at 10% concentration the interaction between impurities is not negligible.

TABLE II. Calculated energies of isolated substitutional impurities, with and without relaxation and extrapolated from molecular-statics calculations.

Impurity	Host	Relaxed (eV)	Unrelaxed (eV)	Extrapolated (eV)
Cu	Ag	0.199	0.348	0.187
Ag	Cu	0.098	0.190	0.113
Au	Ag	−0.211	−0.187	−0.184
Ag	Au	−0.199	−0.191	−0.178
Cu	Au	−0.298	−0.188	−0.255
Au	Cu	−0.280	−0.156	−0.249

VI. CONCLUSIONS

The intention of this work was to show that a simple extension of the FS potential scheme can lead to reasonable potentials for noble-metal alloys that can be used in confidence in studies of extended defects such as grain boundaries and dislocations in these alloys. Throughout, we have adhered to a philosophy of minimizing the amount of empirical refitting and keeping the functional forms as simple as possible. We were aware that compromising this commitment to simplicity, while enabling our results to look more impressive, would have been a pointless exercise because of the inherent simplicity of the FS scheme. As shown here the model describes three distinct types of alloying behavior (ordering, random alloys, and separation) with only a small amount of empirical refitting. Hence, the constructed potentials appropriately describe the structural stability of the alloys as a function of concentration and thus adequately reflect the basic features of the phase diagrams of the alloys studied. At the same time they ensure the mechanical stability of the alloys, leading to correct changes of the lattice parameter and elastic constants with alloying. Both these features are necessary precursors for applicability of these potentials to studies of defective structures where large local deviation from ideal states in both structure and composition are present.

We have also shown that local relaxation is of paramount importance, especially when there is a large difference between atomic sizes of individual species. This will be even more important in defective structures. These features are likely to be reflected appropriately by potentials in whose construction the relaxations were fully incorporated. Also, the differences between the various methods of calculating random-alloying energy show the importance of sampling all possible local configurations; this is especially shown in the differences between the truly random (HCSM) and the average environment (TSM) models. Both of these models describe the relaxation in the same way, so that the errors involved in that approximation, while large, should cancel out when the two models are compared: the only difference comes from the mixing. The significance of the mixing is a feature of the many-body potentials; in a pair-potential model the TSM and HCSM are identical.

We have thus derived a model which maximizes the advantages of many-body empirical potentials over electronic-structure calculations—the speed at which interatomic forces can be calculated, the transparency of the results for interpretation, and the transferability of the energy functions. These potentials should prove useful in applications where atomistic modeling of electronic structure is impractical. The importance of local relaxation and relative unimportance of detailed electronic structure, which have been demonstrated in this paper, suggest that in studies of defective structures more reliable results may be obtained from relaxed molecular-statics or -dynamics calculations than from single-configuration electronic-structure calculations.

ACKNOWLEDGMENTS

This research was supported by the U.S. Department of Energy (Office of Basic Energy Sciences), under Grant No. DE-FG02-87ER45295. The authors would also like to thank Dr. M. W. Finnis for allowing use of his recent improvements to the MOLDY program, and Dr. M. S. Daw and Dr. S. M. Foiles for useful discussions regarding the random alloys.

APPENDIX A: POTENTIALS FOR COPPER, GOLD, AND SILVER

The potentials for gold and silver are the same as those published originally by Ackland *et al.*[17] However, the copper potential used here is the potential rederived for use in molecular-dynamics simulations of radiation damage.[33] The new form eliminates the "bump" in the pair-potential between second and third neighbors. The fitting procedure was identical to that described by Ackland *et al.*[17] except for the choice of knot points in the splines. The extrapolation of the potential to small interatomic separation gives good agreement with the so-called universal equation of states[40] within the range for which that model has been shown to be reasonable.

The form of the potentials is given by Eq. (3) in which r_k^{AA}, R_k^{AA}, and R_{ij} are in units of the corresponding lattice parameters. The lattice parameter a (Å), coefficients a_k^{AA} and A_k^{AA} (eV), and knot points r_k^{AA} and R_k^{AA} (in units of a) are given in Table III.

TABLE III. Parameters of many-body potentials for copper, gold, and silver.

	Copper	Silver	Gold
a	3.615	4.086	4.078
a_1	61.735 258 61	20.368 404	29.059 066
a_2	−108.184 678 00	−102.360 75	−153.147 79
a_3	57.000 539 48	94.312 77	148.178 81
a_4	−12.887 965 78	−6.220 051	−22.205 08
a_5	39.163 819 01	31.080 889	72.714 65
a_6	0.000 000 00	175.560 47	199.262 69
A_1	10.037 183 05	1.458 761	21.930 125
A_2	17.063 632 99	42.946 555	284.996 31
r_1	1.225	1.224 744 9	1.224 744 9
r_2	1.202	1.154 705 4	1.154 705 4
r_3	1.154	1.118 006 5	1.118 006 5
r_4	1.050	1.000 000 0	1.000 000 0
r_5	0.866	0.866 025 4	0.866 025 4
r_6	0.707	0.707 106 8	0.707 106 8
R_1	1.225	1.224 744 9	1.118 006 5
R_2	0.990	1.000 000 0	0.866 025 4

APPENDIX B: CONSTRAINTS IMPOSED ON ELASTIC CONSTANTS

For pure fcc materials the elastic constants are within the FS scheme given as follows:

$$\begin{aligned}
\Omega_0 C_{11} &= 2\sum_j V''(R_j^2)x_j^4 - 2\Phi_0^{-1/2}\sum_j \Phi''(R_j^2)x_j^4 + \Phi_0^{-3/2}\left[\sum_j \Phi'(R_j^2)x_j^2\right]^2 , \\
\Omega_0 C_{12} &= 2\sum_j V''(R_j^2)x_j^2y_j^2 - 2\Phi_0^{-1/2}\sum_j \Phi''(R_j^2)x_j^2y_j^2 - \Phi_0^{-3/2}\left[\sum_j \Phi'(R_j^2)x_j^2\right]^2 , \\
\Omega_0 C_{44} &= 2\sum_j V''(R_j^2)x_j^2y_j^2 - 2\Phi_0^{-1/2}\sum_j \Phi''(R_j^2)x_j^2y_j^2 ,
\end{aligned} \tag{B1}$$

where the coordinate axes x and y are parallel to the cube axes and the summations extend over all the neighbors of the atom i at the origin. $\phi_0=\sum_j \Phi(R_j^2)$, Ω_0 is the atomic volume, and V and Φ are regarded as functions of R^2. For a derivation of these equations, the reader is referred to Ref. 17. These equations can be extended to the alloys assuming homogeneous strain by summing over all possible local configurations as in the LCSM or HCSM:

$$C_{kl}=\sum_\alpha \left[\prod_n \binom{Z_n}{N_n^A} c_A^{N_n^A} c_B^{N_n^B}\right](C_{kl}^A c_A + C_{kl}^B c_B) , \tag{B2}$$

where

$$\begin{aligned}
\Omega_0 C_{11}^A &= 2\sum_j V''_{AT_j}(R_j^2)x_j^4 - 2\Phi_0^{-1/2}\sum_j \Phi''_{AT_j}(R_j^2)x_j^4 + \Phi_0^{-3/2}\left[\sum_j \Phi'_{AT_j}(R_j^2)x_j^2\right]^2 , \\
\Omega_0 C_{12}^A &= 2\sum_j V''_{AT_j}(R_j^2)x_j^2y_j^2 - 2\Phi_0^{-1/2}\sum_j \Phi''_{AT_j}(R_j^2)x_j^2y_j^2 - \Phi_0^{-3/2}\left[\sum_j \Phi'_{AT_j}(R_j^2)x_j^2\right]^2 , \\
\Omega_0 C_{44}^A &= 2\sum_j V''_{AT_j}(R_j^2)x_j^2y_j^2 - 2\Phi_0^{-1/2}\sum_j \Phi''_{AT_j}(R_j^2)x_j^2y_j^2 .
\end{aligned} \tag{B3}$$

Analogous equations apply for C_{11}^B, C_{12}^B, and C_{44}^B. T_j is the subscript identifying species of the atom at site j and $\Phi_0=\sum_j \Phi_{AT_j}(R_j^2)$.

If we define C_{kl}^P to be the pair-potential contribution to the elastic constants, then it follows from Eqs. (B2) and (B3) that $C_{12}^P=C_{44}^P$. This constraint is essentially the same as the Cauchy relations that inhibit pair potentials. We assume here that $\Phi_{AB}=\sqrt{\Phi_{AA}\Phi_{BB}}$, and thus the contributions from the many-body term to the alloy elastic constants are determined entirely by the pure-material fit. Hence, if we were to use alloy elastic constants in fitting V_{AB} (which we do not), we would find that there were only two independent terms to which to fit (for random alloys). This constraint is even stronger in the case of the $L1_2$ structure, where, unless the interactions extend beyond fourth neighbors, the contribution from the (fittable) term V_{AB} is $C_{11}^P-C_{12}^P=C_{44}^P$. A simultaneous least-squares refitting of all alloy and pure-material constants could, of course, be done to produce a best fit to the elastic constants. This method has been adopted, for example, in work on Ni_3Al.[20]

*Present address: Department of Physics, University of Edinburgh, Mayfield Road, Edinburgh EH9 3JZ, Scotland, United Kingdom.

[1]V. Vitek and J. Th. M. DeHosson, in *Computer-Based Microscopic Description of the Structure and Properties of Materials,* Vol. 63 of *Materials Research Society Symposium Proceedings* (MRS, Pittsburgh, PA, 1986), edited by J. Broughton, W. Krakow, and S. T. Pantelides.
[2]M. S. Daw and M. I. Baskes, Phys. Rev. Lett. **50**, 1285 (1983).
[3]M. S. Daw and M. I. Baskes, Phys. Rev. B **29**, 6443 (1984).
[4]M. W. Finnis and J. E. Sinclair, Philos. Mag. A **50**, 45 (1984).
[5]C. C. Matthai and D. J. Bacon, J. Nucl. Mater. **125**, 138 (1984).
[6]J. M. Harder and D. J. Bacon, Philos. Mag. A **54**, 651 (1986).
[7]J. M. Harder and D. J. Bacon, Philos. Mag. A **58**, 165 (1988).
[8]W. Maysenholder, Philos. Mag. A **53**, 783 (1986).
[9]G. J. Ackland and M. W. Finnis, Philos. Mag. A **54**, 301 (1986).
[10]G. J. Ackland and R. Thetford, Philos. Mag. A **56**, 15 (1987).
[11]M. S. Daw, M. I. Baskes, C. L. Bisson, and W. G. Wolfer, in *Modeling Environmental Effects on Crack Growth Processes,* edited by R. H. Jones and W. W. Gerberich (The Metallurgical Society of AIME, Warrendale, PA, 1986).
[12]M. S. Daw and S. M. Foiles, J. Vac. Sci. Technol. A **4**, 1412 (1986).
[13]M. S. Daw and S. M. Foiles, Phys. Rev. B **35**, 2128 (1986).
[14]S. M. Foiles, Phys. Rev. B **32**, 7685 (1985).
[15]M. S. Daw and S. M. Foiles, Phys. Rev. Lett. **59**, 2756 (1987).
[16]S. M. Foiles, Surf. Sci. **191**, 329 (1987).
[17]G. J. Ackland, G. Tichy, V. Vitek, and M. W. Finnis, Philos. Mag. A **56**, 735 (1987).
[18]R. Thetford, Atomic Energy Research Establishment Report No. M 3697, 1988 (unpublished).
[19]F. Ercolessi, E. Tosatti, and M. Parrinello, Phys. Rev. Lett. **57**, 719 (1986).
[20]S. P. Chen, A. F. Voter, and D. J. Srolovitz, Phys. Rev. Lett. **37**, 1308 (1986).
[21]P. C. Clapp, J. A. Rifkin, S. Charpenay, and Z. Z. Yu, in *High Temperature Ordered Intermetallic Alloys,* Vol. 133 of *Materials Research Society Symposium Proceedings,* edited by C. C. Koch, N. S. Stoloff, C. T. Liu, and A. I. Taub (MRS, Pittsburgh, PA, 1989).
[22]D. G. Pettifor, J. Phys. C **19**, 285 (1986).
[23]D. G. Pettifor and R. Podloucky, J. Phys. C **19**, 315 (1986).
[24]A. R. Miedema, P. F. de Chatel, and F. R. de Boer, Physica B+C (Amsterdam) **100B**, 1 (1980).
[25]P. R. Maarleveld, P. R. Kaars, A. W. Weeber, and H. Bakker, Physica B+C (Amsterdam) **142B**, 328 (1986).
[26]S. M. Foiles, M. I. Baskes, and M. S. Daw, Phys. Rev. B **33**, 7983 (1986).
[27]S. M. Foiles and M. S. Daw, J. Mater. Res. **2**, 5 (1987).
[28]K. Terakura, T. Oguchi, T. Mohri, and K. Watanabe, Phys. Rev. B **35**, 2169 (1987).
[29]T. Mohri, K. Terakura, T. Oguchi, and K. Watanabe, Acta Metall. **36**, 547 (1988).
[30]F. Cyrot, J. Phys. Chem. Solids **29**, 1235 (1968).
[31]G. J. Ackland, M. W. Finnis, and V. Vitek, J. Phys. F **18**, L153 (1988).
[32]A. H. MacDonald and R. Taylor, Can. J. Phys. **62**, 796 (1984).
[33]A. Foreman (unpublished).
[34]K. Maeda, V. Vitek, and A. P. Sutton, Acta Metall. **30**, 2001 (1982).
[35]R. Hultgren, R. L. Orr, P. D. Anderson, and K. K. Kelley, *Selected Values of the Thermodynamic Properties of Metals and Binary Alloys* (Wiley, New York, 1963).
[36]M. J. Marcinkowski, N. Brown, and R. M. Fisher, Acta Metall. **9**, 129 (1961).
[37]S. M. L. Sastry and B. Ramaswami, Philos. Mag. **33**, 375 (1976).
[38]W. B. Pearson, *Handbook of Lattice Spacings and Structures of Metals and Alloys* (Pergamon, Oxford, 1967).
[39]R. O. Simmons and H. Wang, *Single Crystal Elastic Constants and Calculated Aggregate Properties: A Handbook* (MIT Press, Cambridge, MA, 1971).
[40]J. H. Rose, J. R. Smith, F. Guinea, and J. Ferrante, Phys. Rev. B **29**, 2963 (1984).